

Shallow water wave spectral characteristics along the eastern Arabian Sea

V. Sanil Kumar*, P.R. Shanas, K. K. Dubhashi

Ocean Engineering, CSIR-National Institute of Oceanography

(Council of Scientific & Industrial Research)

Dona Paula, Goa 403 004 India

*corresponding author Tel: 0091 832 2450 327 Fax: 0091 832 2450 602

email:sanil@nio.org URL: www.nio.org

Abstract

The spectral characteristics of shallow water waves were studied at two locations along the eastern Arabian Sea during 2011. Wave spectra were single-peaked from June to October and predominantly double peaked during the rest of the year. Even though both locations were subjected to open sea conditions, the percentage of single-peaked spectra was large (63%) in the southern location compared to a location 350 km north (46%), because of variation in local winds. Throughout the year, the double-peaked spectra were mostly swell dominated in the southern location. In the northern location, the double-peaked spectra during January to May and December were sea dominated due to the strong local winds blowing from northwest. For the double peaked wave spectra, the average difference between the spectral peaks was 0.11 Hz, and the average ratio of the spectral energy density at the two peaks was 0.5. Significant wave heights up to 4.2 m and a maximum wave height of 7 m were observed during the southwest monsoon period. Fifty percent of the waves recorded had spectral peak wave periods between 6 and 12 s. The narrowest directional spectra were found for waves with 10 to 12 s peak wave periods. Inverse wave age values were biased towards lower values with peaks in the range of 0.2–0.6, indicating a swell-driven wave regime along the eastern Arabian sea.

Key Words: Double peaked spectra, wind-seas, swells, wind waves, mixed sea state

1. Introduction

Wave spectra at specific locations are required for the design of coastal and offshore structures (Chakrabarti 2005). When wind-seas and swells are present, the wave energy spectrum will be multi-peaked, with peaks corresponding to wind-seas and swells (Soares 1991; Hanson and Philips 1999). Along the Indian coast, about 60% of the wave spectra have been observed to be multi-peaked, and the remainder were usually single-peaked when the significant wave height (H_{m0}) was more than 2 m (Kumar et al. 2003). Also, the multi-peaked spectra were mainly swell dominated, with the average value of the ratio of the two spectral peaks around 0.6 and the average value of the difference between peak frequencies around 0.09 Hz. Multi-peaked wave spectra with more wind-sea energy than swell energy were observed off Goa (central west coast of India) at 80 m water depth during 17 to 24 March 1986 (Rao and Baba 1996). A number of semi-empirical spectral models are available for various locations (Chakrabarti 2005). For a fully arisen sea condition the Pierson-Moskowitz spectrum (Pierson and Moskowitz 1964) is used, and for a growing sea state the JONSWAP spectrum (Hasselmann et al. 1973) is used. Dattatri et al. (1977), Narasimhan and Deo (1979), Baba et al. (1989) and Kumar et al. (1994), by analysing the data collected along the west coast of India, each recommended using the Scott spectrum (Scott 1965). Harish and Baba (1986) proposed a PMK spectral model combining the Pierson-Moskowitz (1964) and Kitaigorodskii et al. (1975) spectra for the south-west coast of India. Donelan et al. (1985) have proposed a spectrum with high frequency face proportional to f^4 instead of f^5 . The waves in the north Indian Ocean are high during summer monsoon period (June to August) and the highest H_{m0} measured was 6 m (Kumar et al. 2010). Kumar and Kumar (2008) studied the spectral characteristics of high ($H_{m0} > 2$ m) shallow water waves and found that the measured wave spectrum can be represented by a JONSWAP spectrum with the modified JONSWAP parameters. Glejin et al. (2012) studied the variations in wave parameters along the eastern Arabian Sea, covering a distance of 850 km for 3 months during the summer monsoon, and found that the wave height increases from south to north along the west coast of India.

In the present paper, we studied the wave spectral characteristics during one year at two locations along the eastern Arabian sea that were separated by 50 km. Our study was based on simultaneous measurements carried out at the two locations using moored directional waverider buoys.

1.1 Study area

The first study site is off Honnavar (southern location) at 9 m water depth (geographic position 14.3042° N; 74.3907° E) and the second is off Ratnagiri (northern location) at 13 m water depth (geographic position 16.9801° N; 73.2584° E), both situated in the eastern Arabian Sea (Figure 1).

The distance between Honnavar and Ratnagiri is around 350 km. The distance from the west coast of India are 2.5 km at Honnavar and 2 km at Ratnagiri. The depth contours of 20, 50, 100 and 200 m occur at 10, 30, 75 and 100 km off Honnavar and at 6, 25, 105 and 125 km off Ratnagiri. Along the study area, the coast is exposed to seasonally reversing monsoon winds, with winds from the southwest (SW) direction during the SW (summer) monsoon period (June to September) and from the northeast (NE) during the NE (winter) monsoon period (October to January). The period between NE and SW monsoon is the pre-monsoon period or the fair weather (FW) period. SW monsoon winds are strong, and the annual rainfall of the region is around 3 m. Tides in the region are mixed and are predominantly semi-diurnal. The average tidal range at Karwar, which is 70 km north of Honnavar, is 1.58 m during spring tide and 0.72 m during neap tide (Kumar et al. 2011). At Ratnagiri, the average spring tidal range is about 1.8 m and the neap tidal range is 0.9 m.

2. Materials and methods

Waves were measured using the Datawell directional waverider buoy (Barstow and Kollstad 1991) for the entire year of 2011. The data were recorded continuously at 1.28 Hz and the data for every 30 minutes were processed as one record. The collected time series was subjected to standard error checks for spikes, steepness and constant signals (Haver 1980), and a total of 17421 records at each location were used for further analysis. The wave spectra were obtained through a Fast Fourier transform (FFT). The FFT of 8 series, each consisting of 256 measured vertical elevations of the buoy data, were averaged to obtain the spectrum. The high frequency cut off was set at 0.58 Hz and the resolution was 0.005 Hz. Significant wave height (H_{m0}), which equals $4\sqrt{m_0}$, and the mean wave period (T_{m02}), which equals $\sqrt{m_0/m_2}$, were obtained from the spectral moment. Where m_n is the n^{th} order spectral moment and is given by $m_n = \int_0^{\infty} f^n S(f) df$, $n=0$ and 2 , $S(f)$ is the spectral energy density at frequency f . Period corresponding to the maximum spectral energy, i.e., spectral peak period (T_p), was obtained from the wave spectrum. Mean wave direction (θ_m) and directional width (σ) corresponding to the spectral peak was estimated based on circular moments (Kuik et al. 1988). We also obtained the spectral narrowness parameter (ν), spectral peakedness parameter (Q_p) (Goda 1970), spectral width parameter (ϵ) based on spectral analysis (Cartwright and Longuet-Higgins 1956) and the maximum spectral energy density (E_{max}). A zero-crossing analysis of the surface elevation time series was used to estimate maximum wave height (H_{max}) and the wave period corresponding to H_{max} ($T_{H_{\text{max}}}$). Measurements were made in Coordinated Universal Time (UTC) and the time referred in the paper is UTC. Wave age was estimated as C_p/U , where C_p is the

wave phase speed at peak frequency and U is wind speed. Wind-seas and swells from the measured wave data were separated through a 1-D separation algorithm (Portilla et al. 2009), on the basis of the assumption that the energy at the peak frequency of a swell system cannot be higher than the value of a PM spectrum with the same peak frequency. The algorithm calculates the ratio (γ^*) between the peak energy of a wave system and the energy of a PM spectrum at the same frequency. If γ^* is above a threshold value of 1, the system is considered to represent wind-sea. Otherwise it is taken to be swell. Wind-sea and swell parameters were computed by integrating over the respective spectral parts. To analyse the wind pattern, we reanalysed the zonal and meridional components of the wind speed at 10 m height at 6 hour intervals from NCEP / NCAR (Kalnay et al. 1996). These data were provided by the NOAA-CIRES Climate Diagnostics Center, Boulder, Colorado at <http://www.cdc.noaa.gov/>.

3. Results and discussions

3.1 Wave spectra

The contribution of individual waves with different wave periods can be easily understood from the wave spectrum. During the one year period, the variation in wave spectral energy density was quite large (0.04 to 40.3 m^2/Hz : Figure 2), so the contour plots of normalised wave spectral energy density in frequency-time domain are presented (Figures 3a and 3b). From January to May and from October to December, multi-peaked wind-sea/swell wave spectra were observed and hence the spectral energy density varied across a wide range of frequencies (0.05-0.4 Hz). During the SW monsoon period, the spectra were mainly single-peaked and the spectral energy density was confined to a narrow frequency range (0.08-0.15 Hz). Glejin et al. (2012) found that during the SW monsoon period, the spectral peak was around 0.08 to 0.1 Hz (12 to 10 s) about 72% of the time along the west coast of India. During our study period, the percentage of single-peaked spectra was higher (63%) in the southern location than in the northern location (46%). In the North Atlantic during a storm period, 76% of the analysed data were single-peaked (Aranuvachapun 1987), and the spectra with bimodal structure were about 20 to 25% in the open North Sea and North Atlantic (Soares 1991). Based on the hindcast data covering a period of 10 years from the North Sea, Boukhanovsky et al. (2007) found that single-peaked wind wave spectra prevailed for about 60-65% of the time. In a yearlong study in the Atlantic Ocean off the Southern Brazilian coast, 69% of the wave spectra were single-peaked (Cuchiara et al. 2009).

Chen et al. (2002) observed that swell occurs more than 80% of the time in most of the world's oceans, and wind waves occur most frequently in the mid-latitudes, decreasing to a minimum at the

equator. They identified three “swell pools” in the tropics where the probability of swell was more than 95%. The highest wave conditions occur in the Southern Ocean with average H_{m0} more than 4 m (Hanley et al. 2010). Wolf et al. (2011) found that waves in Liverpool Bay were mainly generated locally within the eastern Irish Sea and that long period swell was absent. The present study indicates that there was a large variation (46 to 63%) in the type of spectra along the eastern Arabian Sea at sites 350 km apart, mainly due to the variation in local winds. The percentage of single-peaked spectra was high (77 to 87%) during the SW monsoon period compared to other seasons (Table 1). During the FW period, the strong local wind and the swells arriving from the Indian Ocean resulted in more double peaked spectra than were observed in other seasons. To examine the predominance of wind-sea and swell, the monthly averaged wave spectra were estimated and are presented in Figure 4. Monthly averaged wave spectra were single-peaked from June to September at both locations, with a similar peak frequency. They were double peaked during the rest of the year. From October onwards, the contribution of wind-sea (influence of local wind) from the NW was higher at the northern location, resulting in wind-sea dominated wave spectra there from December to May, whereas the double-peaked wave spectra at the southern location was predominately swell dominated for all months. Over an annual cycle, only 5.5% of the spectra were wind-sea dominated at the southern location compared to 20% at the northern location (Table 1). Sea breezes created by wind-seas and swells from the south Indian Ocean were responsible for the multi-peaked wave energy spectra at both locations. The secondary peak frequency of the swell dominating the double peaked spectrum was at 1.1 to 4 times the primary peak frequency with an average value of 1.7. Baba et al. (1989) found multiple peaks at 1.5 to 2 times the peak frequency while analysing the weekly collected data during February and June to September in the year 1983 at 15 m water depth off south west coast of India. The annual average value of the difference between the spectral peaks was 0.11 Hz and the average ratio of the spectral energy at two peaks were 0.5. Kumar et al. (2003) found that the average value of the ratio of spectral energy of the two peak was 0.6 and the average value of the difference between the peak frequencies was 0.09 Hz. The peak frequency shifted from low to high during the SW monsoon period and shifted back during the NE monsoon period. There were no waves having a spectral peak period of less than 6 s in the eastern Arabian Sea during the SW monsoon period.

The spectral width (ϵ) and narrowness (ν) parameters varies from 0 to 1, and have smaller values for narrower spectra. In our case, high values of ν (0.8) and ϵ (0.9) was found for narrow-banded spectra (Figure 5a) and low values (0.5 and 0.7) for broad-band spectra (Figure 5d to 5e), indicating that this parameter cannot be used as an indicator for spectral narrowness because ν depends on the second

order moment and is therefore sensitive to the high frequency portion of the spectrum. The spectral peakedness parameter (Q_p) was found to be a good indicator for spectral narrowness, with high values for narrow band spectra (Figures 5a to 5c) and low values for broad band spectra (Figures 5d to 5f). Q_p increases as the bandwidth becomes narrow (fully developed wind-seas have $Q_p \approx 2$, whereas narrow banded swells will have values >2). Goda (1976) has reported Q_p values of 2 to 3 from single-peaked spectra recorded in the Japanese coastal waters. For wind-seas, the spectral peakedness parameter increases with H_{m0} and for swells, the peakedness parameter did not increase with wave height. During the SW and NE monsoon periods, the wave spectra were narrow banded (mean value of $Q_p \approx 2$) and for high waves ($H_{m0} > 2m$), the average value of Q_p was 2.2. During the FW period, the wave spectra were broad banded due to the presence of wind-sea and swell and resulted in lower values of Q_p . Kumar et al. (2010) found that during the onset of the summer monsoon, the value of Q_p varied from 2.5 to 3. Large values of Q_p also indicate that the wave spectrum was narrow banded for high waves. Since the swell is a narrow spectrum, the JONSWAP spectrum (Hasselmann et al. 1973) with appropriate peak enhancement parameter (γ) can represent the swell (Goda 1983). Hence, Kumar and Kumar (2008) could represent the shallow water wave spectrum of high waves ($H_{m0} > 2 m$) with a JONSWAP spectrum with modified parameters. Furthermore, as swell results from a wind-sea that propagates away from the generation area, it is natural that a young swell is described by the same spectral model as wind-sea (JONSWAP). The annual average value of the JONSWAP parameters α (Phillips constant) and γ were 0.0016 and 1.36 for Honnavar and 0.0022 and 1.51 for Ratnagiri. Kumar and Kumar (2008) found that for waves with a H_{m0} more than 2 m, the estimated average value of the JONSWAP parameters, α and γ were 0.0027 and 1.63 and that they were less than the generally recommended values of 0.0081 and 3.3, respectively. Ochi and Hubble (1976) found that the JONSWAP spectrum provided a good approximation to the data for the unimodal spectra with mean JONSWAP parameters of $\alpha = 0.023$ and $\gamma = 2.2$. For high waves ($H_{m0} > 2m$), α and γ were 0.0024 and 1.53 for both locations and were similar to the values reported by Kumar and Kumar (2008). H_{m0} was more than 2 m during 14% of the time at Honnavar and 19% at Ratnagiri. As in an earlier observation (Kumar and Kumar 2008), the SCOTT spectra underestimated the spectral peak.

3.2 Wave direction

Low frequency waves (0.05-0.14 Hz) during January-May approached from 210-240° (Figures 3c and 3d). During the SW monsoon, the waves mainly approached from 240-270°. High frequency waves (>0.14 Hz) were mainly from 270-300° at Honnavar and from 300-330° at Ratnagiri. During

the onset of the SW monsoon, for two days high frequency waves were from 210-240° at both locations. During the SW monsoon at Honnavar, low frequency waves (0.03-0.08 Hz) were from 210-240° but the percentage of waves approaching from 210-240° at Ratnagiri was much lower. During the NE monsoon period, 6-18 s waves were from 210-240° at both locations. The mean direction of 0.1 Hz waves was the same at both locations, whereas the directions of the waves having frequency 0.2 to 0.4 Hz were higher at Ratnagiri than that at Honnavar during January-March and during October-December, indicating the presence of NW waves only at the northern location (Figure 6).

The wind data from offshore of Ratnagiri during January-March and October-December had more NW components and resulted in more NW waves at Ratnagiri. Monthly average wave directions at all frequencies were largely from the SW quarter during June to September at both locations. The mean wave direction with respect to coastal inclination determines the direction of movement of littoral sediments in the near shore region. During the SW monsoon period at both Honnavar and Ratnagiri, waves were predominantly swells arriving from the SW (255°-258°) (Table 2). The average coastal inclination is 17° to the west from the true north at Honnavar. Hence, waves having direction 253° will be approaching perpendicular to the coast (the wave crest angle of these waves will be parallel to the coastline). The average difference in the wave direction of the wind-sea and swell was negligible (2-5°) during the summer monsoon period. In contrast, during the FW and NE monsoon period, the average direction of wind-sea and swell was greater (48 to 64°). The monthly mean wave direction was almost the same during the SW monsoon period at both locations. At other times, there was a large difference in the mean wave direction: at the southern location swells approaching from SW were predominant whereas at the northern location, seas from NW were predominant (Table 2).

We used a near shore wave transformation model to examine the influence of bathymetry on the wave direction measurements at both locations. The Delft3d-wave module developed by WL, delft hydraulics, Netherlands (2011) was used in the study. Computations in Delft3d were based on the wave energy distribution. The domain covering from the 100 m depth contour to the coast was divided into 500 x 500 grid points with 250 m spacing in both the x and y axes. Various cases were considered, with mean wave direction varying from 180 to 360° and peak wave period from 3 to 10 s. The near shore transformed wave characteristics at 9 and 13 m for both locations were extracted and presented as a nomogram (Figure 7). The model showed that, depending on the wave period, waves from 210° in deep water will have a direction of 217-241° at 9 m water depth off Honnavar

and a direction of 212-243° at Ratnagiri (Figures 7a and c). The change in direction from 13 m to 9 m water depth was marginal (<4°) for waves approaching perpendicular to the coast. The change in wave direction from 13 to 9 m water depth was less at Ratnagiri (up to 7°) than that at Honnavar (up to 15°) for the deep water waves at 210° (Figure 7) due to the difference in bathymetry.

3.3 Wave spectral parameters

Significant wave heights up to 4.2 m and maximum wave heights up to 7 m were observed during the study period, and 50% of the waves recorded had a spectral peak wave period between 6 and 12 s. Since the wave spectra were multi-peaked, consisting of both swells and locally generated waves (wind-seas), the swell components and the wind-seas were separated, and the wave parameters of wind-seas and swells are presented in Table 2. The average value of the ratio of the swell height to sea height was the same (1.9) during the southwest monsoon period at both locations. A slight increase (10%) in H_{m0} was found from Honnavar to Ratnagiri during the SW monsoon and FW period (Figure 8a). The increase in H_{m0} in the northern location during the FW period was mainly due to the increase in the height of wind-sea (H_{m0se}). During the SW monsoon, this was due to the combined effect of wind-sea and swell. The average value of the ratio of the swell height to wind-sea height was more than one at the southern location in all seasons, indicating the predominance of swell at this location. In contrast, at the northern location, the average ratio of the swell height to wind-sea height was less than one during the FW period (0.67) and NE monsoon period (0.9), indicating the dominance of wind-seas at this location. The mean wave period at the northern location was relatively shorter than at the southern location (annual average values of 5.1 and 5.6 s), due to the more frequent wind-seas in the northern location (Figure 8b). The difference was large during the FW period and the NE monsoon period, indicating that there is a strong sea breeze in the northern location compared to southern location. T_{m02} varied between 4 and 5 s depending on predominant sea conditions during January to April. The average of the mean wave period (T_{m02}) of sea was 3.6 s at Honnavar and 3.8 s at Ratnagiri and that of swell at both locations were 10.6 and 10.2 s (Table 2). The peak wave period indicates that wave spectra were predominantly swell in the southern location in all the months, whereas in the northern location wind-sea dominated spectra were predominant during January to May and December (Figure 8c), due to the strong local winds. Monthly average spectral energy density was higher in the northern location during the SW monsoon period (Figure 8d) due to the increase in the wave height resulting from the NW swells and SW swells (Glejin et al. 2013).

High waves ($H_{m0} > 3$ m) have spectral peak periods between 9 and 12 s (Figure 9a), and long period swells (14-22 s) with high H_{m0} (2 to 3 m) were also observed. The average ratio of T_{m02} to T_p was 0.8 at Honnavar and 0.79 at Ratnagiri for wind-sea dominated waves, which is close to the ratio of 0.78 previously found for wind-sea (Wolf et al. 2011). Significant steepness [$=2\pi H_{m0}/(g T_{m02} T_{m02})$] varied from 1:18 to 1:283 with higher steepness values (mean steepness 1:48) at Ratnagiri and lower values (mean steepness 1:65) at Honnavar. The higher steepness values at Ratnagiri were due to the higher contribution of wind-seas (54%) in the measured data than at Honnavar (40%). The directional spreading parameter (directional width) at the spectral peak was less than 25° for high waves ($H_{m0} > 2$ m) with average value of 17° for Ratnagiri and 13° for Honnavar. The narrowest directional spectra (directional width $<10^\circ$) was found for waves with periods 10 to 12 s (Figure 9b). Similar to H_{m0} , the maximum spectral energy density was also high for waves with T_p values ranging from 9 to 12 s (Figure 9c). During the FW period, SW and NE monsoon periods, swells contributed 45, 74 and 59% to the measured data at Honnavar, and 28, 73 and 38% at Ratnagiri. The dominance of swells (~ 75 to 79%) along the Arabian sea during the SW monsoon period has been observed in earlier studies (Kumar et al. 2012; Glejin et al. 2012). Even though the wind at the study region was strong during this period, the wind blowing over the entire Arabian Sea was also strong and the waves generated in the Arabian Sea propagate towards the coast. When these swells were added to the wave systems at the measurement location, the energy of the wind-sea was reduced and that of the swell increases (Donelan 1987), to result in dominance of swells. Glejin et al. (2013) found that during the FW and NE monsoon period, the near shore wave characteristics off Ratnagiri were induced by the sea breeze blowing over the region and wave height reaches a maximum value at around 15:00 UTC (09:30 LT). Due to the presence of the sea breeze, the percentage of seas during FW and the NE monsoon period was large (72 and 62) at Ratnagiri. The contribution of short period waves ($T_p < 6$ s; dominated by local seas) was higher (23%) at Ratnagiri than that at Honnavar (4%), whereas the contribution of long period waves ($T_p > 12$ s; results primarily from swell) was higher (47%) at Honnavar and lower (28%) at Ratnagiri. Waves with T_p values greater than 18 s were observed during 3.6% and 2.4% of time at Honnavar and Ratnagiri, and these waves were from the SW. The contributions of intermediate period waves were similar (49%) at both locations.

The water depth is 9 (at Honnavar) and 13 m (at Ratnagiri) at the wave measurement locations. Since the measurement was done in relatively shallow location, the measured waves were influenced by the depth. The average value of the ratio of water depth and wave length associated with the mean wave period was <0.5 (0.23 at Honnavar and 0.35 at Ratnagiri), indicating that the measured waves

were in transitional water. Hence, the waves measured were the transformed waves, and the wave height and the wave direction measured will be different from waves in deep water (Figure 7).

3.4 Wind wave parameters

Wave age indicates the high dominance of swell over wind-sea throughout the year in the region. A decrease in the swell energy and an associated increase in the wind-sea were observed in the FW period. The inverse wave age, the ratio of the surface wind speed to the speed of the waves at the peak of the spectrum (U/C_p), is a good indicator of the degree of coupling between the wind and the waves. High values of inverse wave age indicate regions where the waves are strongly coupled to the local wind field and low values indicate regions where swells are present (Hanley et al. 2010). Histograms of inverse wave age for the study area were biased towards lower values of inverse wave age with peaks in the range of 0.2–0.6, indicating a swell-driven wave regime (Hanley et al. 2010). Off Ratnagiri, locally generated waves [according to Thompson et al. (1984), wave steepness (H_{m0}/L) > 0.025] were observed 55% of the year, whereas off Honnavar they were only observed 41% of the time. The wave age of the measured data was less than 10 for 96% of time, indicating that the waves were young sea with swells. Donelan et al. (1993) proposed that $U/C_p = 0.83$ corresponds to the value of the spectrum at full development, and that the spectral components below this value should be classified as swell and those above it as wind-sea. In the present case, 8% of the waves off Ratnagiri and 18% off Honnavar have inverse wave ages greater than 0.83 (Figure 10), indicating that the pure wind-sea was less along the eastern Arabian Sea, since the waves were measured in open ocean. Based on the data from five field campaigns to study the influence of wave age on the air–sea momentum flux during pure wind-sea conditions, Drennan et al. (2003) found that pure wind-seas were frequent in coastal regions, in enclosed seas, and during extreme wind events. In the open ocean, swell was usually present.

The correlation between U/gT_p and U^2/gH_{m0} (Figure 11) is one method for analysing swell/wind-sea regimes. The dashed line represents the theoretical curve based on following expression for a fully developed wind-sea, as given by Hasselmann et al., (1976).

$$\frac{U}{g T_p} = 4.8 \times 10^{-2} \left(\frac{U^2}{g H_{m0}} \right)^{0.66} \quad (1)$$

The wind-sea from SW and W are mainly under the fully-developed condition (Figure 11). The wind-sea from NW deviates from the theoretical curve for fully developed conditions due to the

short fetch. The year of wave data from off Honnavar and Ratnagiri fall slightly below the theoretical fully developed wind-sea curve due to the presence of swells in the region.

4. Conclusions

Analysing a year of ocean wave data from two shallow-water locations in the eastern Arabian sea shows that during the SW monsoon period, the spectra were mainly single-peaked and that the spectral energy density was confined to a narrow frequency range (0.08-0.15 Hz). Single-peaked spectra were more common (63%) in the southern location compared to the northern location (46%). During the fair weather period, due to the strong local winds and the swells arriving from the Indian Ocean, more double-peaked spectra were observed. The double-peaked spectra were usually swell-dominated in the southern location (Honnavar), whereas in the northern location (Ratnagiri), the double-peaked spectra during January to May and December were usually sea-dominated, indicating the presence of strong local wind from the NW. The contribution of wind-seas in the measured data (54%) was higher at the northern location than in the south (40%). The average difference between the spectral peaks was 0.11 Hz and the average ratio of the spectral energy density at two peaks was 0.5, with a secondary peak frequency 1.7 times the primary peak frequency. Waves having spectral peak periods less than 6 s were not present during the SW monsoon period. During the FW and NE monsoon period, the average difference in wave direction of wind-sea and swell was large (48 to 64°) and therefore it is important to consider the direction of sea and swell while planning marine operations along the west coast of India. The change in wave direction from 13 to 9 m water depth was less at Ratnagiri (up to 7°) than that at Honnavar (up to 15°) due to the difference in near shore bathymetry. The annual average value of the JONSWAP parameters, α and γ were 0.0016 and 1.36 for Honnavar and 0.0022 and 1.51 for Ratnagiri and were much lower than the generally recommended values of 0.0081 and 3.3 respectively. Our data were slightly lower than the theoretical fully developed wind-sea curve, due to the presence of swells in the region. The study shows that there was less pure wind-sea along the eastern Arabian Sea because the waves were measured in open ocean. The narrowest directional spectra was found for waves with periods of 10 to 12 s. The inverse wave ages were biased toward lower values with a peak in the range of 0.2–0.6, indicating a swell-driven wave regime.

Acknowledgments

The authors gratefully acknowledge the financial support given by the Earth System Science Organization, Ministry of Earth Sciences, Government of India to conduct this research. The directors of CSIR-NIO, Goa and INCOIS, Hyderabad provided encouragement to carry out the study. We thank Dr. T. M. Balakrishnan Nair, Head of the Ocean Science & Information Services Group, Indian National Centre for Ocean Information System, Hyderabad for initiating the wave measurements at Ratnagiri. We thank Mr. Arun Nherakkol, a scientist with INCOIS and Mr. Jai Singh, technical assistant at CSIR-NIO, for the help during data collection. The numerical wave transformation presented in the paper is part of the Ph.D. thesis of the second author. This is NIO contribution No. ----.

References

- Aboobacker VM, Vethamony P, Rashmi R (2011) "Shamal" swells in the Arabian Sea and their influence along the west coast of India. *Geophys Res Lett* 38 (3):1-7
- Aranuvachapun S (1987) Parameters of JONSWAP spectral model for surface gravity waves-I. Monte Carlo simulation study, *Ocean Eng* 14:89-115
- Baba M, Dattatri J, Abraham S (1989) Ocean wave spectra off Cochin, west coast of India, *Indian J Mar Sci* 18:106-112
- Barstow SB, Kollstad T (1991) Field trials of the directional waverider, *Proceedings of the First International Offshore and Polar Engineering Conference III*: 55-63
- Boukhanovsky AV, Lopatoukhin LJ, Soares CG (2007) Spectral wave climate of the North Sea, *Applied Ocean Research* 29: 146–154
- Cartwright DE, Longuet-Higgins MS (1956) The statistical distribution of the maxima of a random function, *Proceedings Royal Society of London, A* 237:212-232
- Chakrabarti SK (2005) *Handbook of Offshore Engineering, Vol-1, Ocean Engineering Series, Elsevier*, p 661
- Chen G, Chapron B, Ezraty R, Vandemark D (2002) A global view of swell and wind sea climate in the ocean by satellite altimeter and scatterometer. *J Atmos Ocean Tech* 19:1849–1859
- Cuchiara DC, Fernandes EH, Strauch JC, Winterwerp JC, Calliari LJ (2009) Determination of the wave climate for the southern Brazilian shelf, *Continental Shelf Research* 29: 545–555
- Dattatri J, Jothi Shankar N, Raman H (1977) Comparison of Scott spectra with ocean wave spectra. *J. Waterways Port Coastal and Ocean Eng ASCE* 103:375-378
- Donelan MA (1987) The effect of swell on the growth of wind waves. *Johns Hopkins APL Technical Digest* 8 (1): 18-23

- Donelan MA, Dobsen F, Smith S, Anderson R (1993) On the dependence of sea surface roughness on wave development. *J Phys Oceanogr* 23:2143–2149
- Donelan MA, Hamilton J, Hui WH (1985) Directional spectra of wind generated waves. *Philosophical Transactions of Royal Society, London, A* 315:509-562
- Donelan MA, Hui WH (1990) Mechanics of ocean surface waves. In: Geernaert, G., Plant, W. (Eds.), *Surface Waves and Fluxes*. Kluwer Academic Publishers, The Netherlands, 336p
- Donelan MA, Skafel M, Graber H, Liu P, Schwab D (1992) On the growth rate of wind-generated waves. *Atmosphere–Ocean* 30(3):457–478
- Drennan WM, Graber HC, Hauser D, Quentin C (2003) On the wave age dependence of wind stress over pure wind seas. *J Geophys Res* 108:8062, doi:10.1029/2000JC000715
- Glejin J, Kumar VS, Nair TNB, Singh J (2013) Influence of winds on temporally varying short and long period gravity waves in the nearshore regions of the eastern Arabian Sea, *Ocean Sciences* 9; 343–353
- Glejin J, Kumar VS, Philip CS, Singh J, Pednekar P, Kumar KA, Dora UG, Gowthaman R (2012) Variations in swells along eastern Arabian Sea during the summer monsoon. *Open J Mar Sci* 2:43-50
- Goda Y (1970) Numerical experiments on wave statistics with spectral simulation, in: *Report Port and Harbour Research Institute*. Japan 9:3–57
- Goda Y (1976) “On Wave Groups,” *Proc. Conf. Behaviour of Offshore Structures*, Trondheim, Norway Vol. 1:115-128
- Goda Y (1983) Analysis of wave grouping and spectra of long-travelled swell. Japan: Rep. Port Harbour Res. Inst. 22: p. 3-41
- Hanley KE, Belcher SE, Sullivan PP (2010) A global climatology of wind–wave interaction. *J Phys Oceanogr* 40:1263–1282
- Hanson J L, Phillips OM (1999) Wind sea growth and dissipation in the open ocean. *J Phys Oceanogr* 29: 1633-1648
- Harish CM, Baba M (1986) Spectral and statistical properties of shallow water waves. *J Ocean Eng* 13:239-248
- Hasselmann K, Barnett TP, Bouws E, Carlson H, Cartwright DE, Enke K, Ewing JA, Gienapp H, Hasselmann DE, Kruseman P, Meerburg A, Muller P, Olbers DJ, Richter K, Sell W, Walden H (1973) Measurements of wind-wave growth and swell decay during the Joint North Sea Wave Project (JONSWAP). *Deutsche Hydrograph. Z.* A12,95
- Hasselmann K, Ross DB, Miller P, Sell W (1976) A parametric wave prediction model. *J Phys Oceanogr* 6:200-228
- Haver S (1980) Analysis of uncertainties related to the stochastic modelling of ocean waves. Division of Marine structures, The Norwegian Institute of Technology, Norway, Report No. UR-80-09, pp. 187
- Kalnay E, Kanamitsu M, Kistler R, Collins W, Deaven D, Gandin L, Iredell M, Saha S, White G, Woollen J, Zhu Y, Leetmaa A, Reynolds B, Chelliah M, Ebisuzaki W, Higgins W, Janowiak J, Mo KC, Ropelewski C, Wang J, Roy Jenne, Joseph D (1996) The NCEP/NCAR 40-year reanalysis project. *Bulletin of the American Meteorological Society* 77:437-471

- Kitaigorodskii SA, Krasitskii VP, Zaslavskii MM (1975) On Phillips theory of equilibrium range in the spectra of wind generated gravity waves. *J Phys Oceanogr* 5:410-420
- Kuik AJ, Vledder G, Holthuijsen LH (1988) A method for the routine analysis of pitch and roll buoy wave data. *J Phys Oceanogr* 18:1020–1034
- Kumar VS, Anand NM, Kumar KA, Mandal S (2003) Multi peakedness and groupiness of shallow water waves along Indian coast. *J Coastal Res* 19:1052-1065
- Kumar VS, Dora GU, Philip S, Pednekar P, Singh J (2011) Variations in tidal constituents along the nearshore waters of Karnataka, west coast of India, *J Coastal Res*, 27: 824-827.
- Kumar VS, Johnson G, Dora GU, Philip SC, Singh J, Pednekar P (2012) Variations in nearshore waves along Karnataka, west coast of India. *J Earth Syst Sci* 121:393-403
- Kumar VS, Kumar KA (2008) Spectral representation of high shallow water waves. *Ocean Eng* 35:900-911
- Kumar VS, Mandal S, Anand NM, Nayak BU (1994) Spectral representation of measured shallow water waves. *Proc. Indian National Conference on Harbour and Ocean Engg. (INCHOE-94), CWPRS, Pune India Vol. I: 23-32*
- Kumar VS, Pathak KC, Pednekar P, Raju NSN, Gowthaman R (2006) Coastal processes along the Indian coastline. *Curr Sci India* 91(4):530–536
- Kumar VS, Philip S, Nair TNB (2010) Waves in shallow water off west coast of India during the onset of summer monsoon. *Annales Geophysicae* 28:817-824
- Narasimhan S, Deo MC (1979) Spectral analysis of ocean waves - A study. *Proc. conf. Civil Engineering in Oceans, ASCE* 877-892
- Ochi MK, Hubble EN (1976) On six parameter wave spectra. In proceedings 15th Coastal Engineering Conference, ASCE 321-328
- Pierson WJ, Moskowitz L (1964) A proposed form for fully developed seas based on the similarity theory of S.A. Kitaigorodski. *J Geophys Res* 69:5181-5190
- Portilla J, Ocampo-Torres FJ, Monbaliu J (2009) Spectral Partitioning and Identification of Wind Sea and Swell. *J Atmos Ocean Tech* 26:pp.117-122
- Rao CVKP, Baba M (1996) Observed wave characteristics during growth and decay: a case study. *Continental Shelf Res* 16(12): 1509-1520
- Scott JR (1965) A sea spectrum for model test and long-term ship prediction. *J ship res* 9:145-152
- Soares CG (1991) On the occurrence of double peaked wave spectra. *Ocean Eng.* 18(1/2):167-171
- Thompson TS, Nelson AR, Sedivy DG (1984) Wave group anatomy. in: *Proceeding of 19th conference on Coastal engineering, American Society of Civil Engineers*, 1, 661–677
- WL Delft Hydraulics (2011) *Delft3d User Manual*. Delft. The Netherlands www.oss.delft3d.nl
- Wolf J, Brown JM, Howarth MJ (2011) the wave climate of Liverpool Bay—observations and modelling. *Ocean Dyn* 61:639–655

Figure Captions

Figure 1 Study area showing the two locations (Honnavar and Ratnagiri) where waves were measured

Figure 2 Time history of maximum spectral energy density during 2011 at both locations

Figure 3 Contour plots of normalised spectral energy density at Honnavar (a) and Ratnagiri (b), and mean wave direction at Honnavar (c) and Ratnagiri (d) during 2011

Figure 4 Monthly averaged wave spectra in different months for both locations

Figure 5 Typical single-peaked and multi-peaked wave spectra

Figure 6 Monthly averaged mean wave direction in different months

Figure 7 Wave direction at 100 m water depth and the corresponding direction at 13 and 9 m water depth at Honnavar and Ratnagiri

Figure 8 The monthly average value of (a) significant wave height, (b) mean wave period, (c) peak wave period (d) maximum spectral energy density and (e) mean wave direction

Figure 9 Variation of (a) significant wave height, (b) directional width and (c) maximum spectral energy density with peak wave period at Honnavar and Ratnagiri

Figure 10 Percentage of inverse wave age (U/C_p)

Figure 11 Plot of $\log(U/gT_p)$ versus $\log(U^2/gH_{m0})$ stratified by peak wave direction (SW, W and NW) for wind-sea and for all the data measured at Honnavar and Ratnagiri. Dashed line represents the theoretical relation given by Eq. 1.

Table 1: Percentage of single-peaked, swell-dominated and sea-dominated wave spectra during different periods at Honnavar and Ratnagiri

Location	Type of wave spectra	SW monsoon	NE monsoon	FW period (pre monsoon)	Annual
Honnavar	Single Peaked spectra	87.5	60	42.0	63.0
	Swell dominated multi peaked spectra	12.5	34	47.5	31.5
	Sea dominated multi peaked spectra	0.0	6	10.5	5.5
Ratnagiri	Single Peaked spectra	77.7	36	25.0	46.0
	Swell dominated multi peaked spectra	22.3	38	39.8	34.0
	Sea dominated multi peaked spectra	0.0	26	35.2	20.0

Table 2: Average value of wave parameters at Honnavar and Ratnagiri during 2011

Parameter	Honnavar			Ratnagiri		
	FW period (Pre monsoon)	SW monsoon	NE monsoon	FW period (Pre monsoon)	SW monsoon	NE monsoon
H_{mo} (m)	0.7	1.8	0.6	0.8	2.0	0.6
H_{max} (m)	1.0	2.8	0.9	1.2	3.2	0.9
H_{m0sw} (m)	0.5	1.6	0.4	0.4	1.7	0.3
H_{m0se} (m)	0.5	0.9	0.3	0.6	1.0	0.4
T_{m02} (s)	4.8	6.5	5.6	4.4	6.4	4.7
T_{m02sw} (s)	11.5	9.4	10.9	11.0	9.1	10.6
T_{m02se} (s)	3.5	3.9	3.5	3.7	4.0	3.6
T_{Hmax} (s)	9.1	9.6	10.0	6.6	8.9	7.6
T_p (s)	12.4	11	12.4	9.4	10.7	10.1
θ_m (deg)	239	255	234	270	258	262
θ_{sea} (deg)	291	260	276	299	260	300
θ_{swell} (deg)	229	255	228	240	258	236
σ (deg)	26.5	15.1	27.0	26.9	19.2	29.2
ν	0.61	0.53	0.64	0.53	0.51	0.54
ε	0.77	0.81	0.81	0.71	0.80	0.74
Q_p	1.7	2.0	1.9	1.8	2.0	1.9
E_{max} (m^2/Hz)	0.64	5.5	0.59	0.60	6.4	0.38
U/C_p	0.39	0.82	0.40	0.39	0.64	0.38

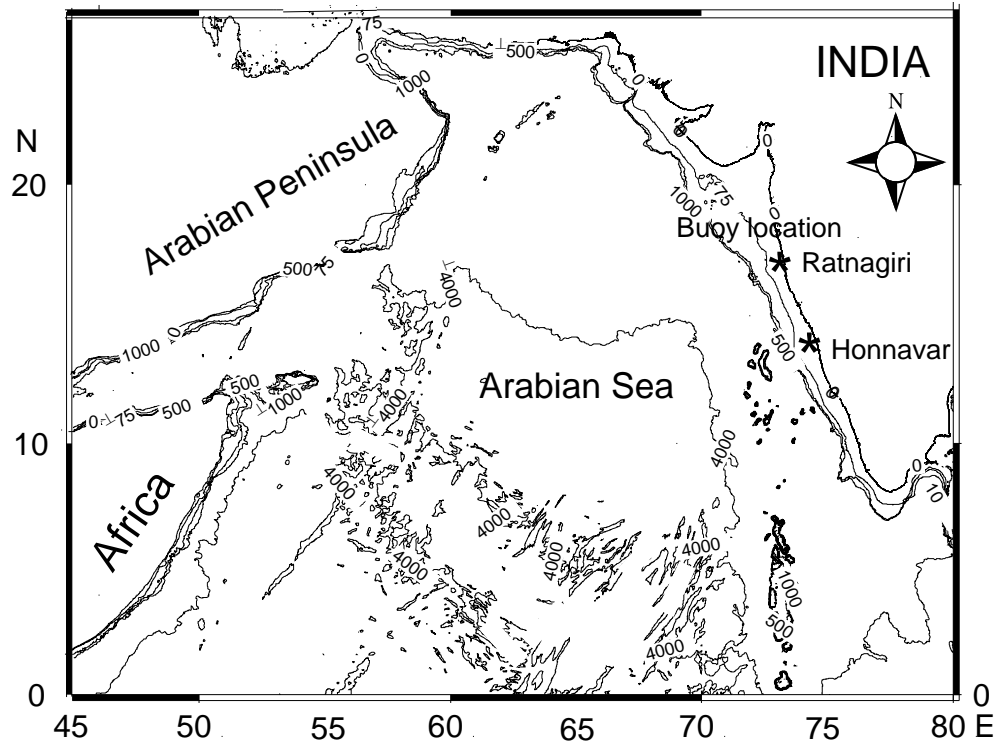


Figure 1 Study area showing the two locations (Honnavar and Ratnagiri) where waves were measured. The depth contours are in meters.

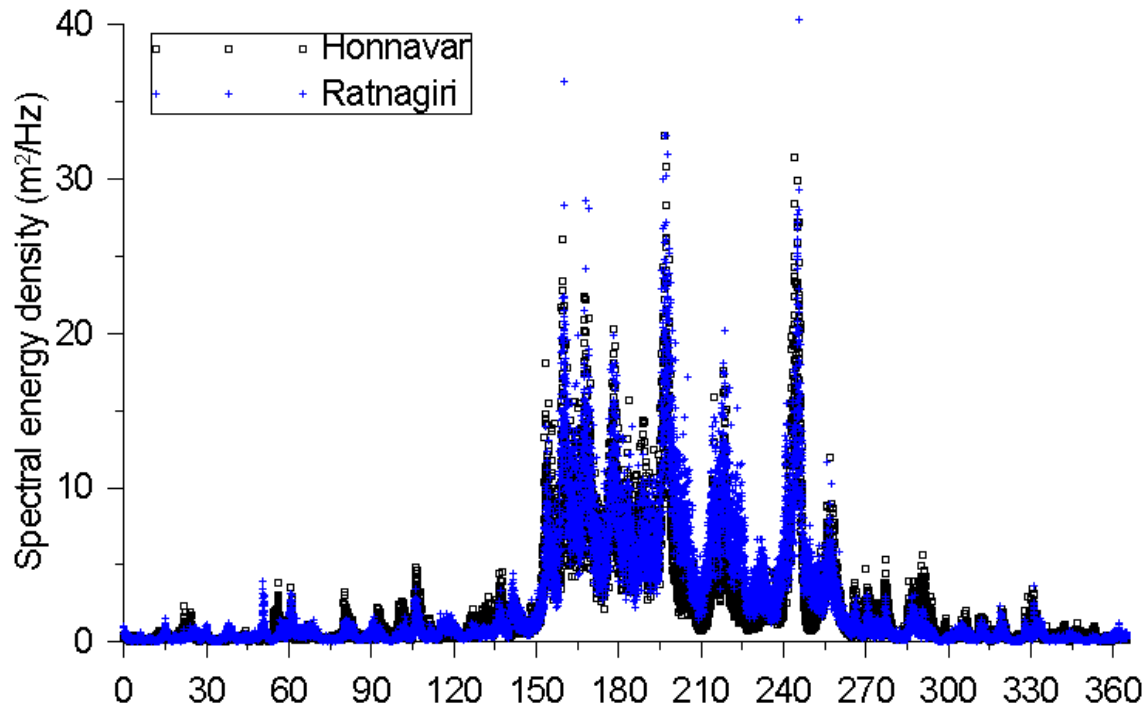


Figure 2: Time history of maximum spectral energy density during 2011 at both locations

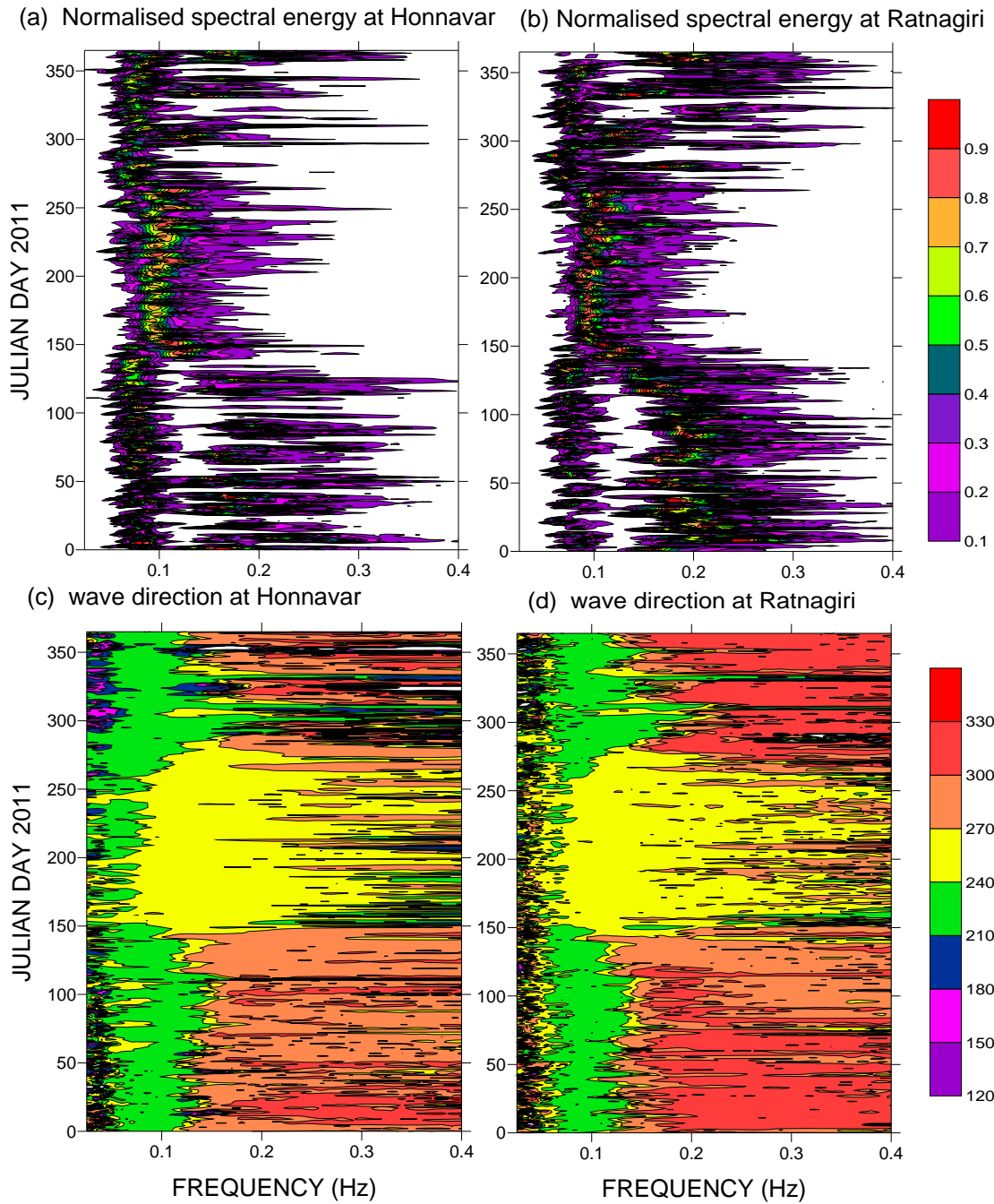


Figure 3 Contour plots of normalised spectral energy density at Honnavar (a) and Ratnagiri (b), and mean wave direction at Honnavar (c) and Ratnagiri (d) during 2011

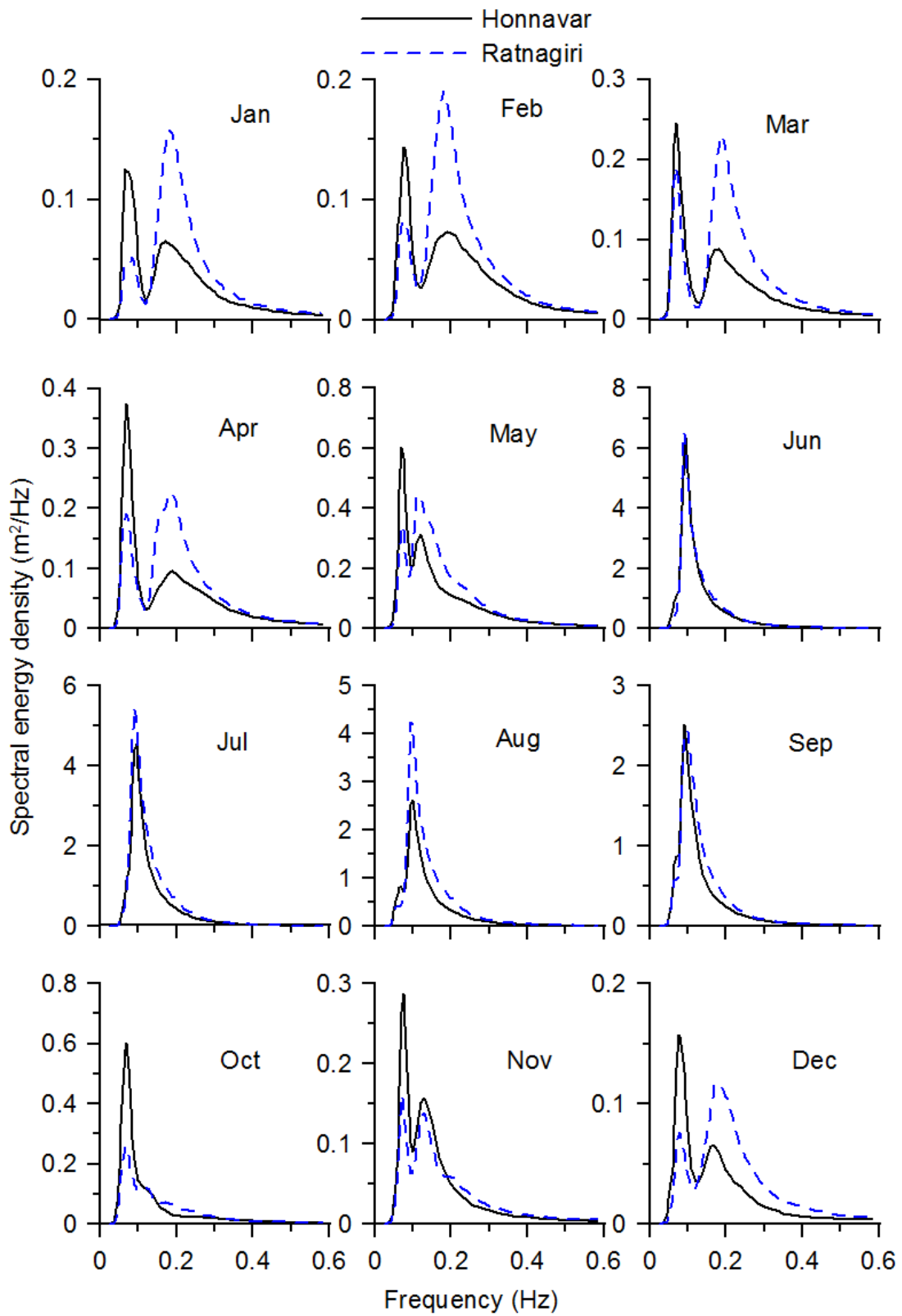


Figure 4: Monthly averaged wave spectra in different months for both locations

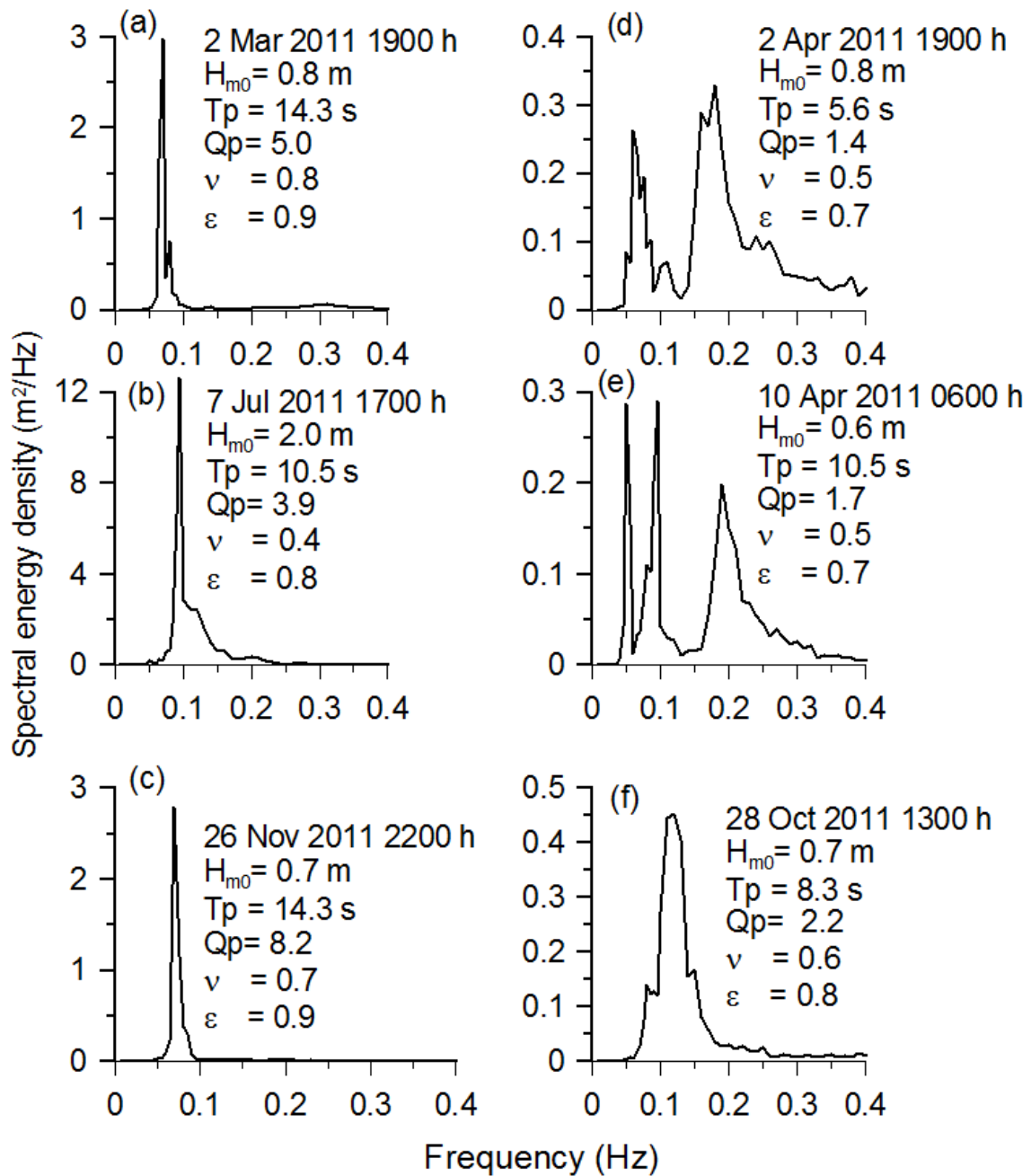


Figure 5: Typical single-peaked and multi-peaked wave spectra

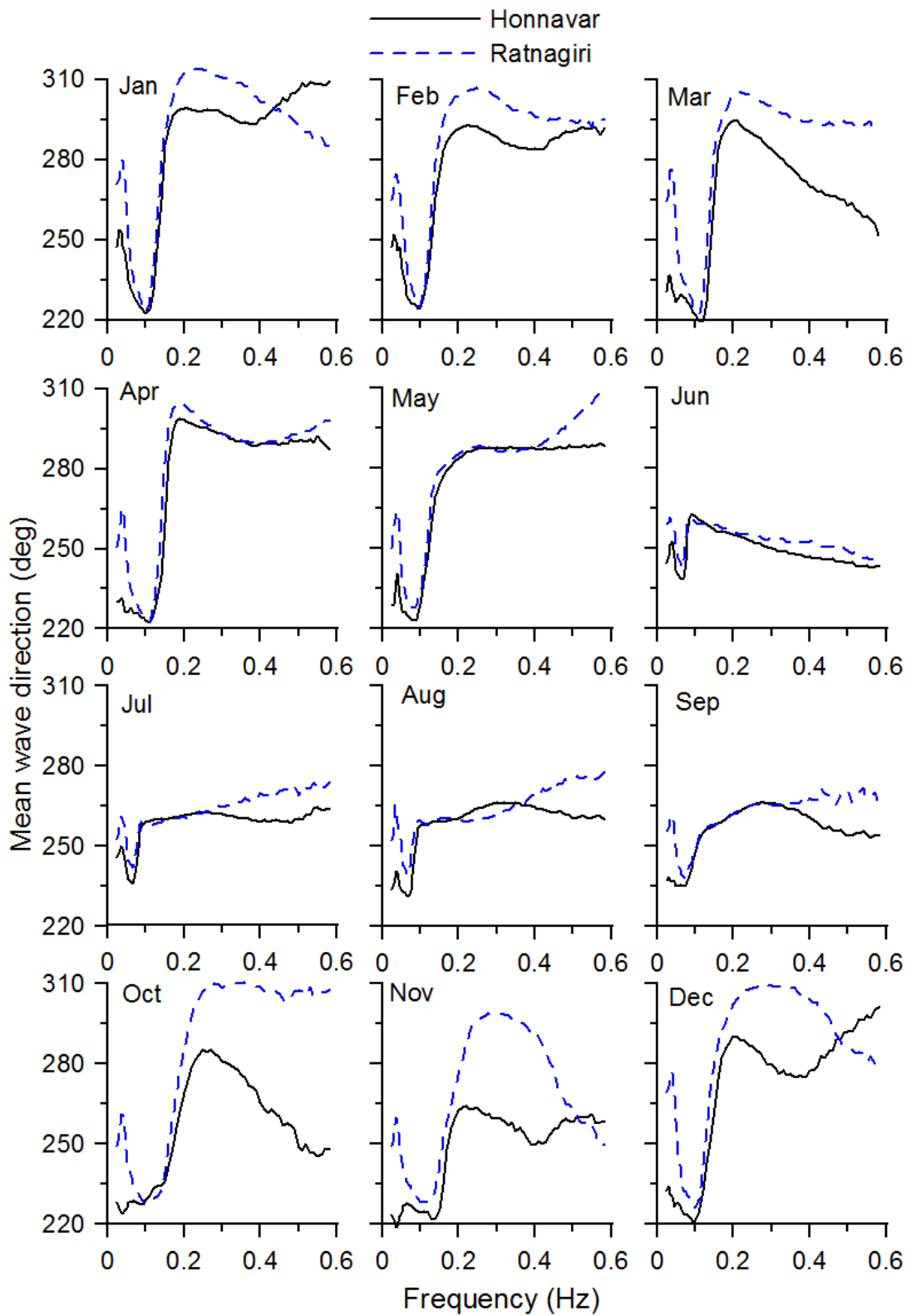


Figure 6: Monthly averaged mean wave direction in different months

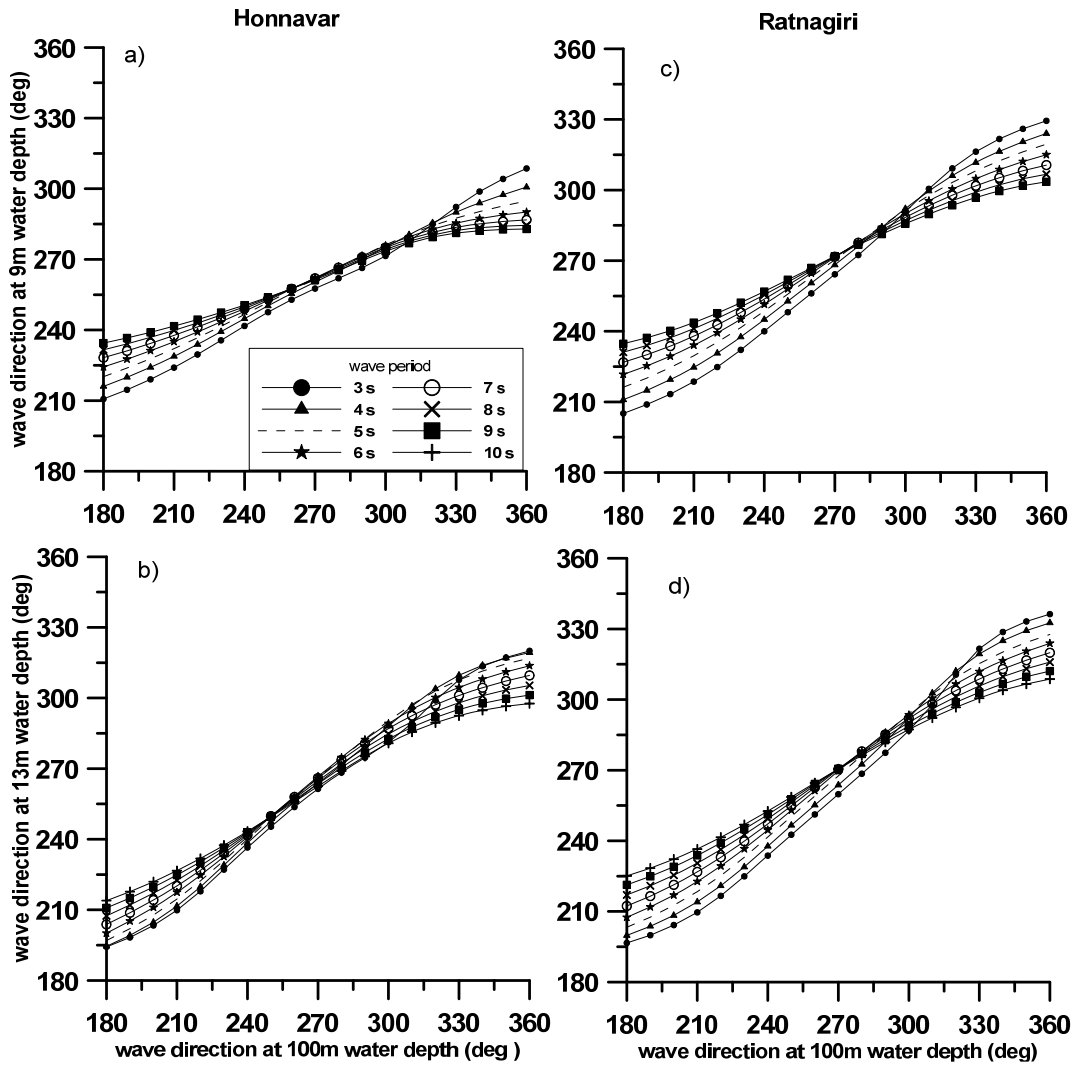


Figure 7: Wave direction at 100 m water depth and the corresponding direction at 13 and 9 m water depth at Honnavar and Ratnagiri

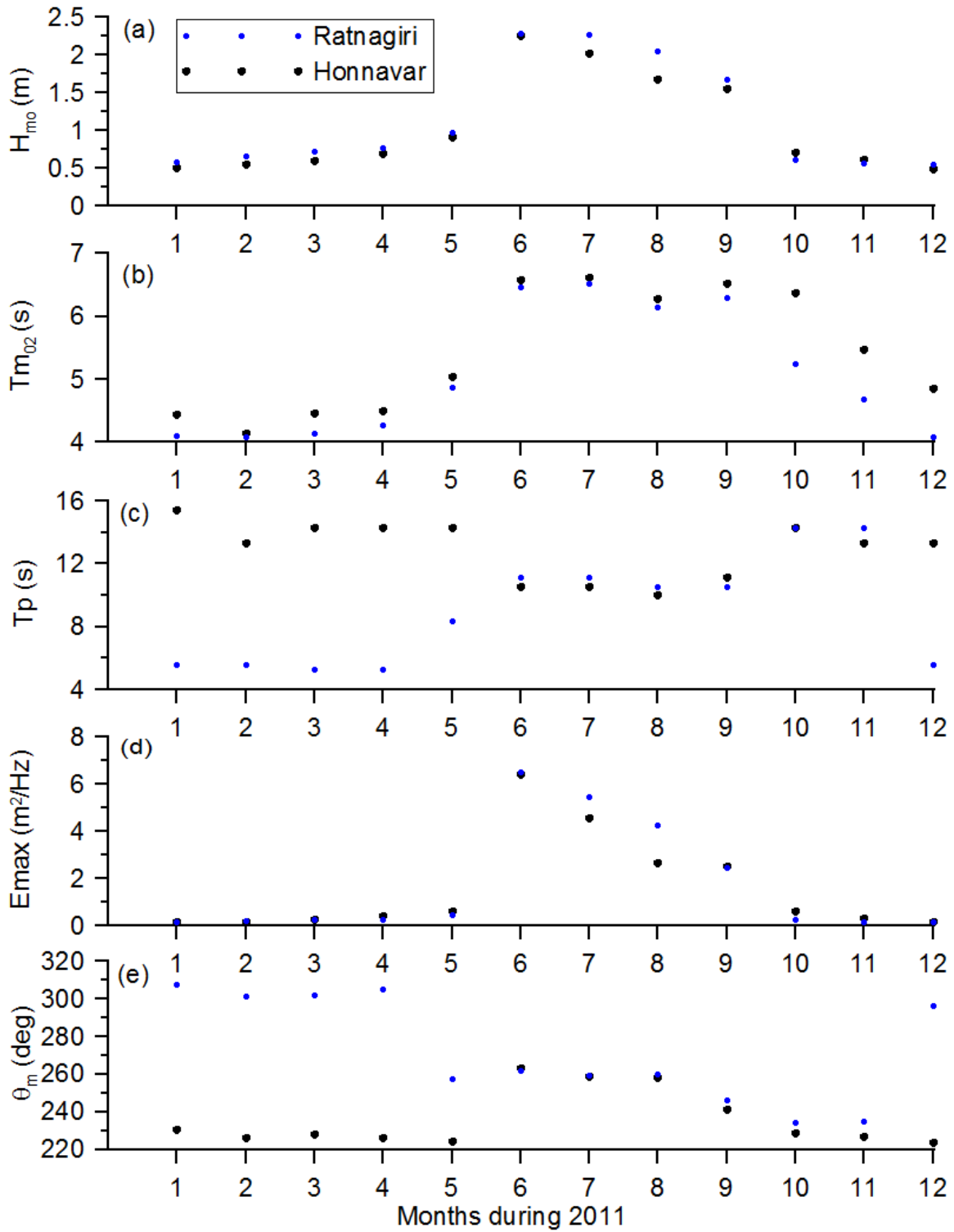


Figure 8: The monthly average value of (a) significant wave height, (b) mean wave period, (c) peak wave period (d) maximum spectral energy density and (e) mean wave direction

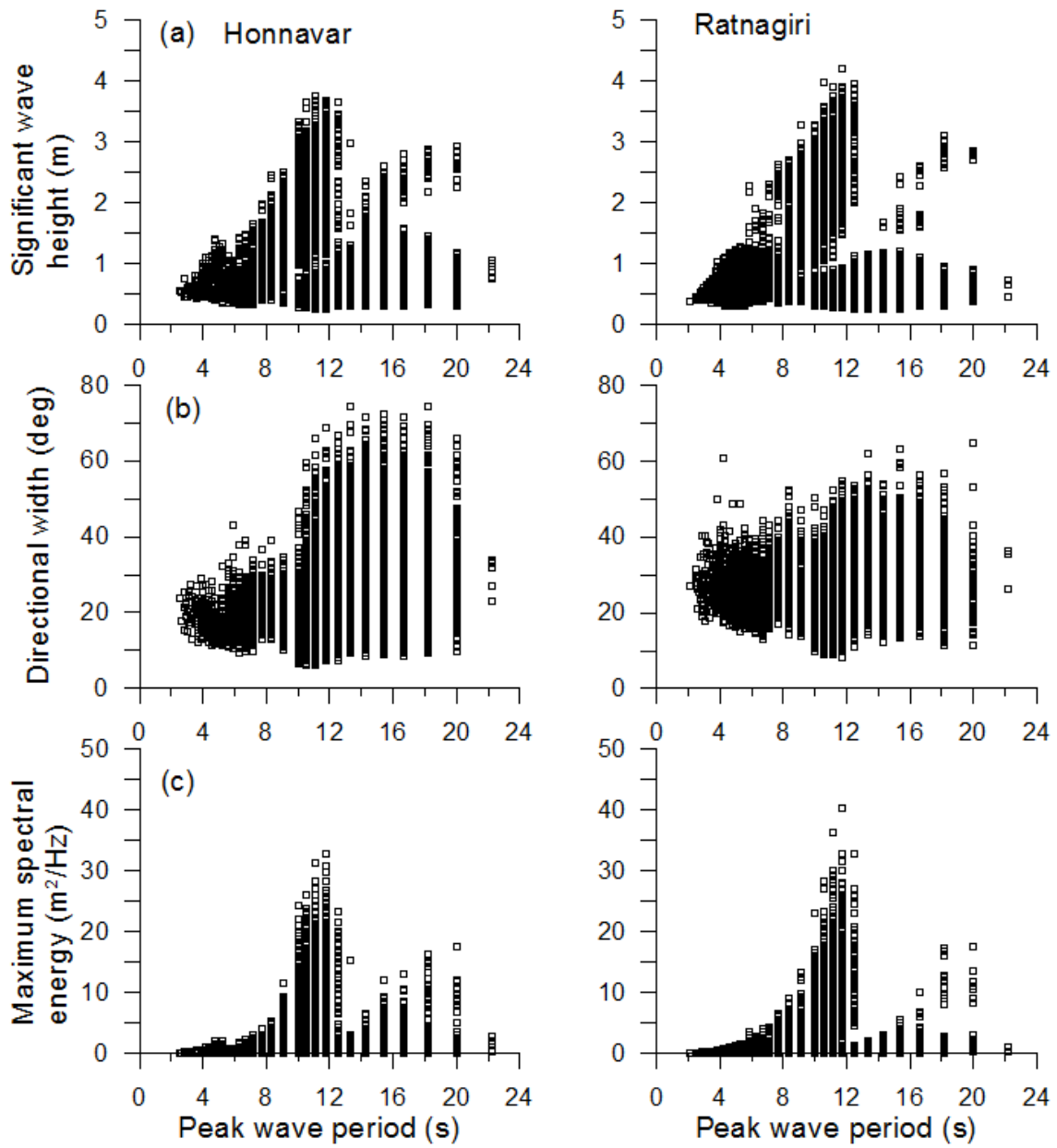


Figure 9: Variation of (a) significant wave height, (b) directional width and (c) maximum spectral energy density with peak wave period at Honnavar and Ratnagiri

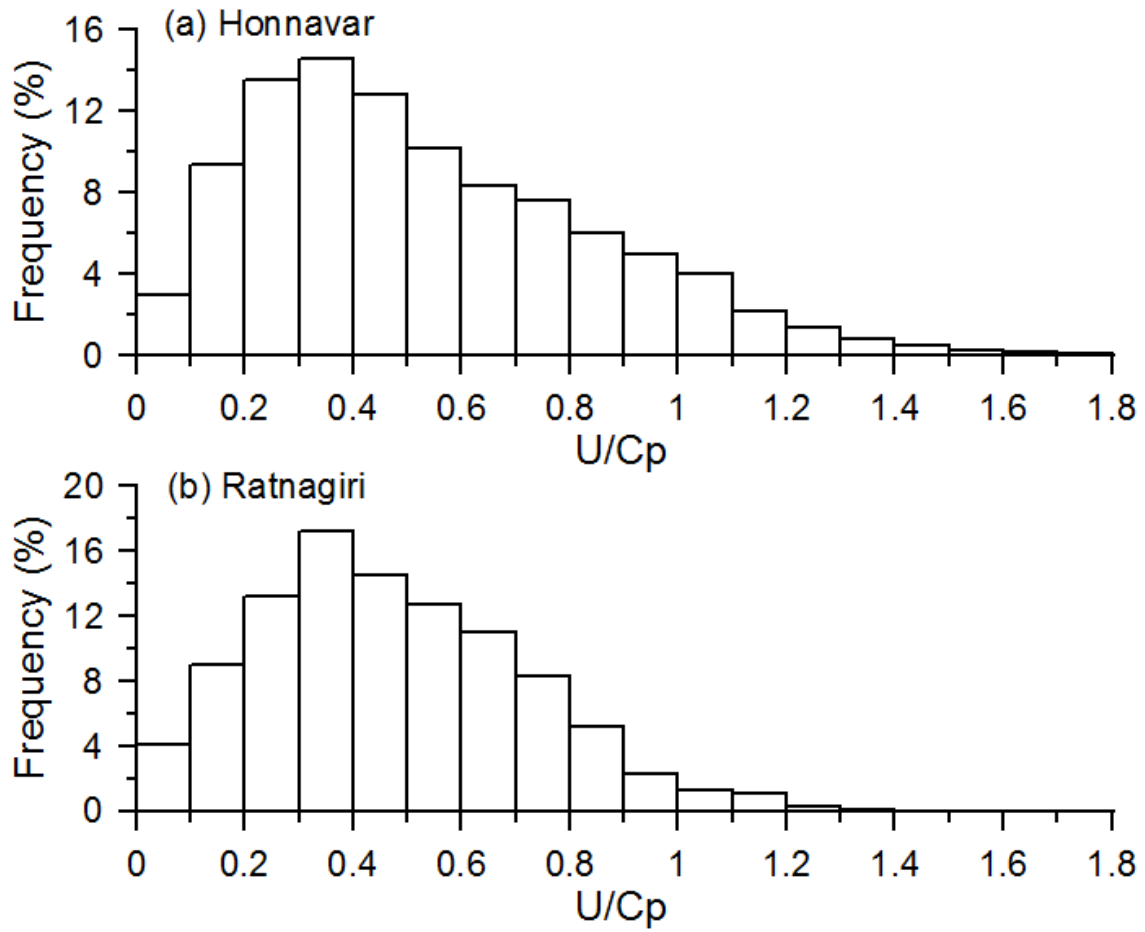


Figure 10: Percentage of inverse wave age (U/C_p)

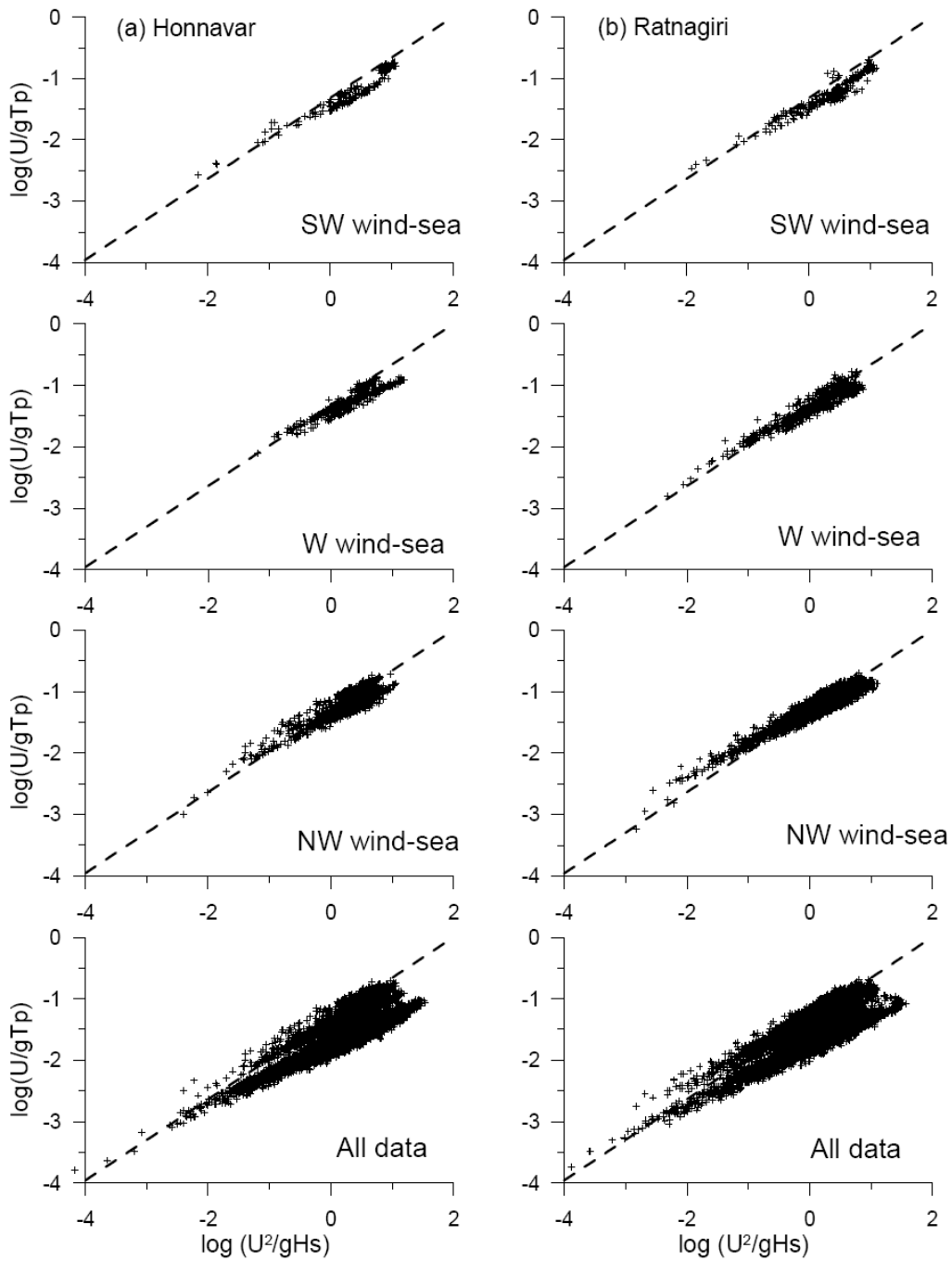


Figure 11: Plot of $\log(U/gT_p)$ versus $\log(U^2/gH_{m0})$ stratified by peak wave direction (SW, W and NW) for wind-sea and for all the data measured at Honnavar and Ratnagiri. Dashed line represents the theoretical relation given by Eq. 1.